Proceedings Paper:

Braitor, A.-C. orcid.org/0000-0002-7666-0457, Konstantopoulos, G. and Kadirkamanathan, V. (2020) Novel droop control design for overvoltage protection of DC microgrids with a constant power load. In: Proceedings of the 28th Mediterranean Conference on Control and Automation (MED'2020). 28th Mediterranean Conference on Control and Automation (MED'2020), 15-18 Sep 2020, Saint-Raphaël, France. IEEE , pp. 875-880. ISBN 9781728157436

https://doi.org/10.1109/MED48518.2020.9182891

Novel droop control design for overvoltage protection of DC microgrids with a constant power load

A.-C. Braitor, G. C. Konstantopoulos and V. Kadirkamanathan

Abstract— **A novel droop controller for DC microgrid systems, consisting of multiple paralleled sources feeding a constant power load (CPL), is proposed to achieve the desired voltage regulation and accurate load power distribution, while ensuring an overvoltage protection for each source. CPLs are well-known to exhibit negative impedance characteristic due to their nonlinear behaviour, which may cause instability to a DC microgrid if the necessary impedance inequality criteria are not satisfied. In this paper, a new droop control scheme is proposed to limit the voltage of each source below a desired bound, achieve tight voltage regulation and power sharing, and guarantee closed-loop system stability with the existence of a CPL. The upper limit of the voltage of each source is rigorously proven using ultimate boundedness theory, while after a suitable manipulation of the admittance matrix of the microgrid, analytic conditions of stability are obtained to guide the control parameters design. To validate the theoretical design and analysis, a detailed simulation is performed of a DC microgrid equipped with the proposed controller.**

I. INTRODUCTION

Following the recent developments in the distributed integration of small-scale power generation combined with intelligent control and coordination of distribution networks, the microgrid concept has been formed, representing a key solution for future power distribution systems. In this framework, extensive research has already been carried out and is still ongoing to devise and enhance the features of the future microgrid systems [1]. With the ever-increasing demand for power and the dire necessity for harnessing green energy resources, microgrids are drawing a deeper interest in the power network industry.

DC microgrids are mostly preferred to AC microgrids as they facilitate seamless integration of renewable resources into the power grids with increased efficiency and flexibility [2]. Therein, the distributed generation (DG) sources are commonly connected in a parallel configuration to a common DC bus. The interface between the DGs and the bus is ensured by power electronic devices, which are responsible to regulate the DC bus voltage and control the output power. These tasks are ordinarily achieved, at the primary control layer, by droop-based methods [3].

In general, droop controllers are utilised in microgrids where communication networks are not suitable for data exchange due to distributed physical locations of the DG sources, with the condition that the line impedances are mainly inductive [4], [5]. However, conventional droop control strategies present some serious shortcomings, such as poor voltage regulation due to their permanent offset, inaccuracies in the load power sharing, dependency on line impedance, slow dynamic response, and low stability margin [6]. The latter aspect is of major significance, especially in the presence of CPLs. Unlike passive loads, CPLs, also known as active loads, enable the power conditioning at the load side and behave as negative impedances in the small-signal analysis, thus, introducing instabilities in the system [7], [8]. To increase the system stability margin, several methods have been proposed in the literature, i.e. passive damping [9] in the form of RC parallel, RL parallel, RL series, additional filter or energy storage devices [10] to deal with the voltage oscillations at the DC bus, virtual resistance [11] to adjust the current flowing through the source and DC link, virtual capacitance [12] to reduce the size and weight of DC-link capacitor. However, to guarantee small-signal stability with a CPL, the impedance inequality criteria must be satisfied.

Apart from the theoretical analysis, the need of protecting the power units from overvoltages via the control design has emerged [13], [14], since DC capacitors are commonly used at the output of each unit's converter, which introduce a maximum limit. Overvoltage instances occur when the voltage in a circuit, or part of the circuit, increases above its designed limit, causing potential damages and faults in the converter components or the grid. Limitations and challenges in dealing with such situations have been discussed in [15]. In [16], a comparison, by means of optimal power flow, between centralized and local voltage control solutions have been conducted to mitigate the voltage rise impact. Other methods, such as those proposed in [17], [18], aim to reduce the active power injected by a source until their voltage complies with the operational requirements, commonly referred to as active power curtailment (APC). In [19], the authors propose a methodology to identify and locate transient overvoltages using wavelet packet decomposition (WPD) and general regression neural networks (GRNN) theory. Still, incorporating the overvoltage protection at the primary control layer remains an open problem.

Therefore, in this paper, a novel primary droop control strategy is employed that ensures an upper bound for the voltages of each source of the DC microgrid and also achieves load voltage regulation and accurate power sharing. The voltage limitation is rigorously proven based on nonlinear ultimate boundedness theory, while the stability

This work was supported by EPSRC under Grant EP/S001107/1.
The authors are with the Department of Automatic Control and Systems Engineering, The Univesity of Sheffield, Sheffield S1 3JD, U.K. G. C. Konstantopoulos is with the Department of Electrical and Computer Engineering, University of Patras, Rion 26500, Greece. {abraitor1,g.konstantopoulos,visakan}@sheffield.ac.uk

of the closed-loop system with a CPL is analytically proven, leading to useful conditions for the control parameter design.

The remainder of this section revisits some notations used throughout the entire manuscript. Section II introduces the DC microgrid model in the presence of a CPL. In Section III, the novel droop control strategy is proposed which includes a useful guideline for selecting the control parameters. Asymptotic stability of the entire microgrid is guaranteed in Section IV, while in Section V the dynamic response of the system states is presented. Conclusions are drawn in Section VI.

A. Common notations

Given an n-dimensional sequence $(v_1, v_2, \ldots, v_n)$, let $v \in \mathbb{R}^n$ represent the associated vector, and $[v] \in \mathbb{R}^{n\times n}$ the associated matrix, whose diagonal entries are the elements of v. Consider $\mathbf{1}_n \in \mathbb{R}^n$ and $\mathbf{0}_n \in \mathbb{R}^n$ being the n-dimensional vector, and $\mathbf{1}_{n\times n} \in \mathbb{R}^{n\times n}$ and $\mathbf{0}_{n\times n} \in \mathbb{R}^{n\times n}$ the n-dimensional matrix with all the entries equal to one, and zero, respectively. Let $\mathcal{I}$ be the ordered index set, and I_n the square identity matrix of size n. For $v \in \mathbb{R}^n$, define the column vector-valued, and diagonal matrix-valued functions $\mathbf{sin}v$, $\mathbf{cos}v$, and $[\mathbf{sin}v]$, $[\mathbf{cos}v]$, respectively.

II. DC MICROGRID MODEL

A common DC microgrid architecture is depicted in Figure 1, consisting of n power converters that have an output capacitor, C_i, and are connected to a common bus, through a line with resistance, R_i, in a parallel configuration and feeding a common load. The dynamic equations of the capacitor voltages can be obtained by employing Kirchhoff's laws

$$C_i \dot{V}_i = i_{ini} - i_i \tag{1}$$

where V_i is the output voltage, and i_{ini} and i_i represent the input and output current respectively. The term i_{ini} also describes the control input, for $\forall i \in \mathcal{I}$. Note that the configuration represents just a generic model of n-sourced units that could be incorporated within the microgrid via different power converter configurations (buck, boost, buck-boost, AC/DC).

In the presence of a CPL, the power balance equation must hold:

$$P = V_o \sum_{i=1}^{n} i_i \tag{2}$$

where V_o is the voltage of the DC bus, and P is the power of the load. The output current i_i then has the following expression:

$$i_i = \frac{V_i - V_o}{R_i}. \tag{3}$$

Now for system (1)-(3), consider the following assumption:

Assumption 1. Let the inequality:

$$\left(\sum_{i=1}^{n} \frac{V_i}{R_i}\right)^2 > 4P \sum_{i=1}^{n} \frac{1}{R_i}$$

hold, with $P > 0$, and $V_i > 0$, $\forall i \in \mathcal{I}$.

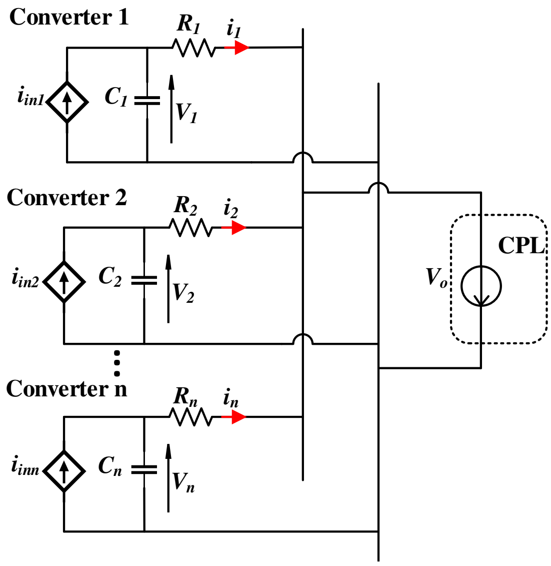

Fig. 1: Generic framework of a DC microgrid

Replacing i_i from (3) into (2), it yields the following expression for the load voltage, given by the real solutions of the second order polynomial as:

$$V_o = \frac{\sum_{i=1}^{n} \frac{V_i}{R_i} \pm \sqrt{\left(\sum_{i=1}^{n} \frac{V_i}{R_i}\right)^2 - 4P\sum_{i=1}^{n} \frac{1}{R_i}}}{2\sum_{i=1}^{n} \frac{1}{R_i}}. \tag{4}$$

The load voltage has two solutions, a high voltage and a low voltage, with the high voltage being the feasible solution.

By taking the partial derivative of the output current, i_i, from (3) with respect to the capacitor voltage, V_i, we get the admittance matrix, Y, similar to [20], as

$$Y = R^{-1}\left(I_n - \mathbf{1}_{n\times n} D\right) \tag{5}$$

with $R = diag\{R_i\}$, and $D = diag\left\{\frac{\partial V_o}{\partial V_i}\right\} \succ 0$ with the following expression

$$D = \frac{1}{2\sum_{i=1}^{n} \frac{1}{R_i}} \left(R^{-1} + \frac{\sum_{i=1}^{n} \frac{V_i}{R_i}}{\sqrt{\left(\sum_{i=1}^{n} \frac{V_i}{R_i}\right)^2 - 4P\sum_{i=1}^{n} \frac{1}{R_i}}} R^{-1} \right)$$

where, according to *Assumption 1*, the denominator $\sqrt{\left(\sum_{i=1}^{n} \frac{V_i}{R_i}\right)^2 - 4P\sum_{i=1}^{n} \frac{1}{R_i}}$ yields a real number. Hence, the positive eigenvalues of D will have the form

$$\lambda_{Di} = \frac{1}{2\sum_{i=1}^{n} \frac{1}{R_i}} \left(\frac{1}{R_i} + \frac{\sum_{i=1}^{n} \frac{V_i}{R_i}}{\sqrt{\left(\sum_{i=1}^{n} \frac{V_i}{R_i}\right)^2 - 4P\sum_{i=1}^{n} \frac{1}{R_i}}} \frac{1}{R_i} \right),$$

with $i \in \mathcal{I}$.

III. PROPOSED CONTROL ARCHITECTURE

The main tasks of the proposed control method are to achieve voltage regulation close to the rated value, and accurate power sharing among the sources with an inherent overvoltage protection for each source independently.

A. Droop control design with overvoltage protection

Inspired by the sl-PI controller in [21], the novel droop control strategy defines the control input, i_{ini}, in the following form

$$i_{ini} \;\; = \;\; -g_i V_i + I_i^{max} sin\sigma_i \tag{6}$$

with σ designed to follow the nonlinear dynamics

$$\dot{\sigma}_i = \frac{k_i}{I_i^{max}}(V^* - V_o - m_i i_i)cos\sigma_i \tag{7}$$

that incorporates the droop control, with V^* representing the reference voltage and m_i the droop coefficient satisfying

$$m_i < R_i, \forall i \in \mathcal{I}. \tag{8}$$

By replacing the controller dynamics into the open-loop system, one gets

$$C_i \dot{V}_i = -g_i V_i + I_i^{max} sin\sigma_i - i_i. \tag{9}$$

Consider the following continuously differentiable energy-like function

$$W_i = \frac{1}{2} C_i V_i^2 \tag{10}$$

and by taking the time derivative, it becomes

$$\begin{aligned} \dot{W}_i \;\; &= \;\; -g_i V_i^2 + V_i I_i^{max} sin\sigma_i - V_i i_i \\ &= \;\; -g_i V_i^2 + V_i I_i^{max} sin\sigma_i - P_i, \end{aligned} \tag{11}$$

where $P_i = V_i i_i$ represents the power fed by the $i-$th source to the common DC bus through each $i-$th line. Depending on the sign of the power P_i, the discussion follows around two separate cases:

a) Case 1: $P_i \geq 0$

From equation (11), one can clearly notice that

$$\dot{W}_i \leq -g_i V_i^2 + V_i I_i^{max} sin\sigma_i \leq -g_i |V_i|^2 + I_i^{max} |V_i|. \tag{12}$$

Let $g_i = \bar{g}_i + \epsilon_i > 0$, with $\bar{g}_i > 0$ and ϵ_i representing an arbitrarily small positive constant. In that case, (12) becomes

$$\begin{aligned} \dot{W}_i \;\; &\leq \;\; -\left(\bar{g}_i + \epsilon_i\right)|V_i|^2 + I_i^{max}|V_i| \\ &\leq \;\; -\epsilon_i |V_i|^2, \, \forall \, |V_i| \geq \frac{I_i^{max}}{\bar{g}_i}. \end{aligned} \tag{13}$$

According to (13), the solution $V_i\left(t\right)$ is uniformly ultimately bounded, and every solution starting with the initial condition $V_i\left(0\right)$, satisfying

$$|V_i\left(0\right)| \leq \frac{I_i^{max}}{\bar{g}_i}, \tag{14}$$

will remain in this range for all future times, i.e.

$$|V_i\left(t\right)| \leq \frac{I_i^{max}}{\bar{g}_i}, \, \forall \, t \geq 0. \tag{15}$$

To ensure that each voltage V_i is bounded below a maximum voltage V^{max}, the control parameters, $\bar{g}_i$ and I_i^{max} can be selected to satisfy

$$\frac{I_i^{max}}{\bar{g}_i} = V^{max}. \tag{16}$$

This completes the design of the control parameters $\bar{g}_i$ and I_i^{max}, to guarantee an upper bound for the output voltage V_i, when $P_i \geq 0$.

b) Case 2: $P_i < 0$

Due to the microgrid structure and the existence of a constant power load, with $P > 0$, at least one current source (e.g. j-th source) should be feeding the CPL and/or other (up to $n-1$) source units. Hence, if the corresponding power of that particular source is $P_j > 0$, then since $P_j = V_j i_j = V_j \frac{V_j - V_o}{R_j}$, it yields that $V_j > V_o$, and equivalently from *Case 1*, there is $V_o < V_j \leq V^{max}$. However, since for the $i-$th source, the output power is negative $P_i = V_i \frac{V_i - V_o}{R_i} < 0$, then $V_i < V_o$ which leads to $V_i < V^{max}$.

Therefore, in both cases, an upper bound for the output voltage is guaranteed, i.e. $V_i(t) \leq V^{max}$, at any time instant, i.e. even during transients.

B. Parameter selection

It should be noted that the controller parameters I_i^{max} and $g_i = \bar{g}_i + \epsilon_i$ can take any values that satisfy (16) in order to guarantee the desired voltage limitation. However, in order to provide a guidance for the user to select these two values, a worst case scenario is considered where the $i-$th source feeds the load by itself, i.e. $P_i \approx P$. In this case, one can easily understand from (11) that depending on the value of P, compared to the term $g_i V_i^2$, the actual upper bound of V_i can be limited well below V^{max}. Given a known upper value of the CPL power, i.e. $0 < P \leq P_{max}$, and since it is desired the upper value of V_i to be as close to V^{max} as possible, one can achieve this by suitably selecting the parameter g_i such that the term $g_i V_i^2$ dominates the term P in (11), i.e. it is at least 10 times higher, in the worst case scenario, hence

$$g_i \geq \frac{10 P_{max}}{(V^{max})^2}. \tag{17}$$

Subsequently, since according to (16) there is $\bar{g}_i V^{max} = I_i^{max}$, then I_i^{max} can be then selected as

$$I_i^{max} \approx \frac{10 P_{max}}{V^{max}}, \tag{18}$$

due to the very small positive constant ϵ_i. Note that the above expressions for selecting the controller parameters are provided for guidance only, since any other selection that satisfies (16) will still guarantee the desired upper bound for each voltage V_i. In addition, a more detailed analysis on the condition that the parameter g_i needs to satisfy is provided in the sequel and is related to the asymptotic stability of the closed-loop system.

IV. Stability analysis

Before beginning the stability analysis of the closed-loop system, the two following lemmas should be introduced first:

Lemma 1. Consider A and B two Hermitian matrices, with $\lambda_1 \leq \lambda_2 \leq \cdots \leq \lambda_n$ the eigenvalues of A, and $\beta_1 \leq \beta_2 \leq \cdots \leq \beta_n$ the eigenvalues of B. Then, the following inequality holds

$$\lambda_i + \beta_1 \leq \eta_i \leq \lambda_i + \beta_n$$

where η_i, with $i \in \mathcal{I}$, represent the eigenvalues of the Hermitian matrix $A+B$.
Proof. in Chapter 7, in [22].

Lemma 2. With S a real symmetric matrix, and D a positive-definite real symmetric matrix, the following statements hold:

1) SD (or DS) is diagonalizable.
2) SD (or DS) has only real eigenvalues, and also the same number of positive, negative or null eigenvalues as matrix S has.

Proof. SD is similar to the symmetric matrix $D^{\frac{1}{2}}SD^{\frac{1}{2}}$, hence diagonalizable. Statement 1) is proved. By polar decomposition SD (or DS) is of the form $SD = UP$, with U unitary and $P = \sqrt{(SD)^T SD}$ a positive-semidefinite symmetric matrix. Consider Q unitary that satisfies $Q^2 = U$. Note that $M = Q^{-1}(SD)Q = QPQ$ is symmetric, and by spectral decomposition $M = V\Lambda V^{-1}$, with V unitary and Λ diagonal with the eigenvalues of M (and same index of inertia as SD) on the main diagonal. One can infer that $(QV)^{-1}SD(QV) = \Lambda$, with QV unitary.

Matrix $D^{\frac{1}{2}}SD^{\frac{1}{2}}$ is congruent with S, hence, according to Sylvester's law of inertia, $D^{\frac{1}{2}}SD^{\frac{1}{2}}$ has the same index of inertia as matrix S. Statement 2) is proved in Chapter 7, in [22].

Now that the necessary lemmas have been stated, let the closed-loop system (7), (9) be written in a matrix form as

$$\dot{V} = C^{-1}\left(-gV + I_{max}\mathbf{sin}\sigma - i\right) \quad (19)$$
$$\dot{\sigma} = I_{max}^{-1}k\left[\mathbf{cos}\sigma\right]\left(\left(V^* - V_o\right)\mathbf{1}_n - mi\right) \quad (20)$$

where $C = diag\{C_i\}$, $V = [V_1 \dots V_n]^T$, $g = diag\{g_i\}$, $I_{max} = diag\{I_i^{max}\}$, $i = [i_1 \dots i_n]^T$, $\sigma = [\sigma_1 \dots \sigma_n]^T$, $k = diag\{k_i\}$, $m = diag\{m_i\}$.

Considering an equilibrium point (V_e, σ_e) of the closed-loop system (19)-(20), (3) and (4), with $\sigma_{ie} = \left(-\frac{\pi}{2}, \frac{\pi}{2}\right)$, that satisfies *Assumption 1*, the following theorem can be formulated that guarantees stability of the entire droop-controlled DC microgrid with a CPL.

Theorem 1. The equilibrium point (V_e, σ_e) is asymptotically stable if the controller parameter g_i satisfies

$$g_i > \frac{n\lambda_{Di} - 1}{R_i}, \forall i \in \mathcal{I}. \quad (21)$$

Proof. The corresponding Jacobian matrix of system (19)-(20) has the following form

$$J = \begin{bmatrix} -C^{-1}g - C^{-1}Y & C^{-1}I_{max}\left[\mathbf{cos}\sigma_e\right] \\ -I_{max}^{-1}k\left[\mathbf{cos}\sigma_e\right]\left(\mathbf{1}_{n\times n}D + mY\right) & \mathbf{0}_{n\times n} \end{bmatrix}$$

Replacing Y from (5), one gets

$$J = \begin{bmatrix} -C^{-1}\left(g - R^{-1}(I_n - \mathbf{1}_{n\times n}D)\right) & C^{-1}I_{max}[\mathbf{cos}\sigma_e] \\ -I_{max}^{-1}k[\mathbf{cos}\sigma_e]\left(\mathbf{1}_{n\times n}D + mR^{-1}(I_n - \mathbf{1}_{n\times n}D)\right) & \mathbf{0}_{n\times n} \end{bmatrix},$$

with the characteristic polynomial of the system given as

$$|\lambda I_{2n} - J| = |\lambda^2 I_n + \lambda\mathbb{C} + \mathbb{K}| = 0, \quad (22)$$

where the two matrix coefficients are

$$\mathbb{C} = C^{-1}g + C^{-1}R^{-1}\left(I_n - \mathbf{1}_{n\times n}D\right)$$
$$\mathbb{K} = C^{-1}\left[\mathbf{cos}\sigma_e\right]^2 k\left(\left(I_n - mR^{-1}\right)\mathbf{1}_{n\times n}D + mR^{-1}\right).$$

By right multiplication with $|D^{-1}| > 0$, equation (22) becomes

$$|\lambda^2 D^{-1} + \lambda\bar{\mathbb{C}} + \bar{\mathbb{K}}| = 0 \quad (23)$$

with

$$\bar{\mathbb{C}} = C^{-1}gD^{-1} + C^{-1}R^{-1}\left(D^{-1} - \mathbf{1}_{n\times n}\right)$$
$$\bar{\mathbb{K}} = C^{-1}\left[\mathbf{cos}\sigma_e\right]^2 k\left(\left(I_n - mR^{-1}\right)\mathbf{1}_{n\times n} + mR^{-1}D^{-1}\right)$$

By left multiplying (23) with $|RC| > 0$, it yields

$$|\lambda^2 RCD^{-1} + \lambda\mathbb{C}^* + \mathbb{K}^*| = 0 \quad (24)$$

with

$$\mathbb{C}^* = RgD^{-1} + D^{-1} - \mathbf{1}_{n\times n}$$
$$\mathbb{K}^* = R\left[\mathbf{cos}\sigma_e\right]^2 k\left(I_n - mR^{-1}\right)\times \left(\mathbf{1}_{n\times n} + \left(I_n - mR^{-1}\right)^{-1}k^{-1}\left[cos\sigma\right]^{-1}R^{-1}mD^{-1}\right)$$

Notice that matrix $\mathbb{C}^*$ is a symmetric matrix, and, after factorisation, matrix $\mathbb{K}^*$, according to *Lemma 2*, is a diagonalizable matrix with real eigenvalues. Thus, by expressing the latter as $\mathbb{K}^* = P^{-1}\Lambda P$, with matrix P being unitary, and Λ diagonal, and replacing it in (24), it yields that

$$|\lambda^2 RCD^{-1} + \lambda\mathbb{C}^* + P^{-1}\Lambda P| = 0 \quad (25)$$

or, equivalently,

$$|\lambda^2 PRCD^{-1}P^{-1} + \lambda P\mathbb{C}^*P^{-1} + \Lambda| = 0 \quad (26)$$

which is a quadratic eigenvalue problem (QEP) with matrix Λ having the same index of inertia as matrix $\mathbb{K}^*$, whereas the similarity transformations $PRCD^{-1}P^{-1}$ and $P\mathbb{C}^*P^{-1}$ are symmetric, since P is unitary $\left(P^{-1} = P^T\right)$, and they have the same eigenvalues as matrices RCD^{-1}, and $\mathbb{C}^*$, respectively. According to the QEP theory, if RCD^{-1}, $\mathbb{C}^*$, and Λ are positive-definite, then the eigenvalues λ will be real and negative, i.e. $\lambda < 0$, thus, J will be Hurwitz.

Since $RCD^{-1} \succ 0$, the remaining conditions are $\mathbb{C}^* \succ 0$, and $\Lambda \succ 0$, or equivalently $\mathbb{K}^*$ has positive eigenvalues.

1) $\mathbb{C}^* \succ 0$: As $\mathbb{C}^*$ is a sum of symmetric matrices, according to *Lemma 1*, the condition becomes
$$\frac{R_i g_i + 1}{\lambda_{Di}} - n > 0, \; i \in \mathcal{I}$$
which is always guaranteed, provided (21) holds.
2) $\Lambda \succ 0$ (or equivalently, $\mathbb{K}^*$ has positive eigenvalues): Due to the choice in (8), and for the bounded $\sigma_{ie} \in \left(-\frac{\pi}{2}, \frac{\pi}{2}\right)$, the first matrix term in the multiplication inside $\mathbb{K}^*$ is positive-definite, i.e.
$$R\left[\mathbf{cos}\sigma_e\right]^2 k\left(I_n - mR^{-1}\right) \succ 0.$$
Therefore, according to *Lemma 2*, one can investigate only the remaining symmetric matrix in the product, which is
$$\mathbf{1}_{n\times n} + \left(I_n - mR^{-1}\right)^{-1}k^{-1}\left[\mathbf{cos}\sigma_e\right]^{-1}R^{-1}mD^{-1}.$$

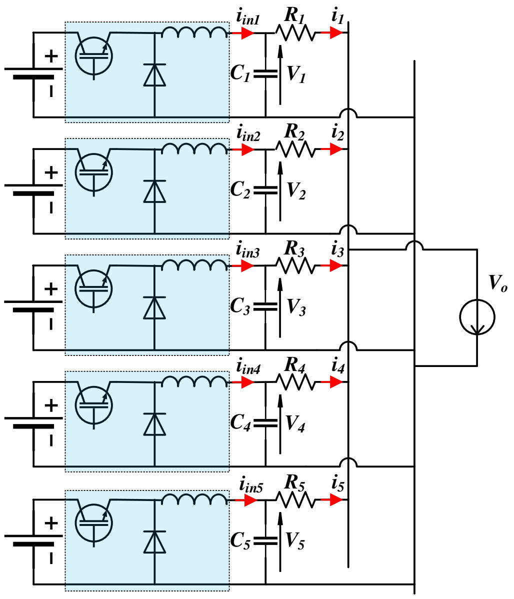

Fig. 2: DC microgrid considered for testing

The above matrix is represented by a sum between a positive semi-definite and a positive-definite symmetric matrices, hence, one can clearly agree that the matrix is positive-definite (*Lemma 1*).

As a result, when (21) is satisfied, J is Hurwitz, and the equilibrium point (V_e, σ_e) is asymptotically stable. This completes the proof.

V. Simulation Results

A DC microgrid portrayed in Figure 2, with the parameters specified in Table I, consisting of five DC/DC buck converters, is simulated in MATLAB/Simulink, considering a $0.3\,s$ testing scenario. The desired task for the proposed controller is to regulate the load voltage close to the reference value, $V^* = 100\,V$, and accurately distribute the load power among converters in a $5:4:3:2:1$ ratio, while maintaining a safe output voltage margin below $1.05V^*$, i.e. $5\,\%$ above the rated value.

The simulation starts at $t = 0\,s$, with a load power demand being $P = 250\,W$. As one can notice in the time responses in Figure 3, the load voltage is tightly regulated very close to the reference with $V_o \approx 99.95\,V$, as expected by the droop control function (Figure 3b). The output currents are accurately shared in a $5:4:3:2:1$ ratio with $i = [0.66\ 0.53\ 0.4\ 0.26\ 0.13]\ A$, as it can be seen in Figure 3a. Note that the output voltages are kept below their upper limit.

Later on, at $t = 0.1\,s$, the load power demand increases to $P = 1\,kW$. Notice that the transient occurring shortly after the load change, at $0.1\,s$, is successfully limited below $105\,V$. As one can see in Figure 3b, the load voltage is still kept very close to the rated with $V_o \approx 99.7\,V$, and the power sharing is also very accurate with the output current vector being $i = [3.34\ 2.67\ 2\ 1.34\ 0.67]\ A$, as displayed in Figure 3a.

At $t = 0.2\,s$, the load power demand increases further to $P = 1.25\,kW$. According to Figure 3b, the new steady-state value of the load voltage is $V_o = 99.6\,V$, meanwhile the output voltage of the 5th DC/DC buck converter is limited below the upper bound $V^{max} = 105\,V$. On the other hand, the power sharing among the other four converters is kept in a $4:3:2:1$ ratio with the output current vector being $i = [3.6\ 2.7\ 1.8\ 0.9]\ A$ as shown in Figure 3a. Hence, the theoretic analysis has been clearly verified, illustrating how the proposed controller has as its first priority to protect each converter by limiting the output voltage below a desired upper bound at all times, while also ensuring the

TABLE I: System and control parameters

System Parameters	Values
$C_{1\ldots5}\ [\mu F]$	[25 50 20 20 5]
$R_{1\ldots5}\ [\Omega]$	[1 1.1 1.05 1.12 1.5]
Control Parameters	**Values**
$m_{1\ldots5}$	[0.42 0.21 0.14 0.105 0.084]
$I^{max}_{1\ldots5}$	[1.05 1.05 1.05 1.05 1.05] $\times$ 6000
$g_{1\ldots5}$	[1 1 1 1 1] $\times$ 60
$k_{1\ldots5}$	[2 2 2 2 38] $\times$ 10^7

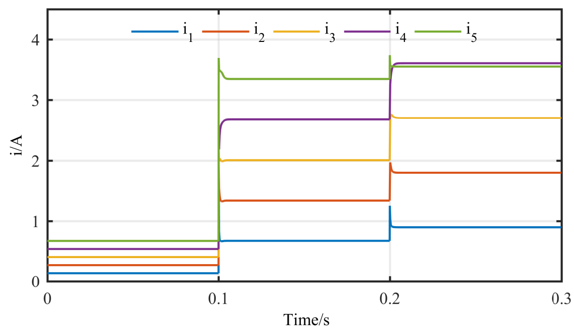

(a) Output currents

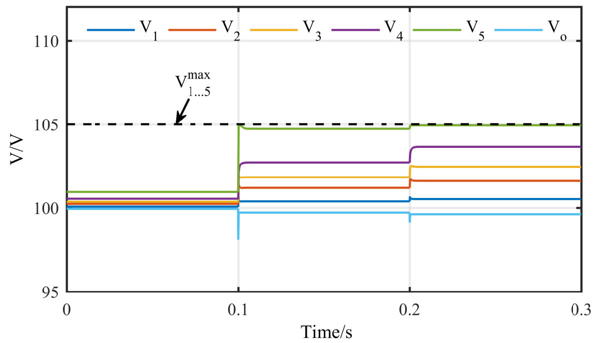

(b) Output voltages

Fig. 3: Simulation results of the DC microgrid equipped with the proposed controller

required power sharing and load voltage regulation in the DC microgrid loaded by a CPL.

VI. Conclusions

In this paper, a novel droop controller with overvoltage protection has been presented. Using nonlinear systems theory, an ultimate bound for the voltage of each source is analytically proven. Following the proposed control strategy, closed-loop asymptotic stability is also guaranteed with a suitable selection of the controller parameters. Simulation testing has been carried out for a DC microgrid consisting of five parallel-operated DC/DC buck converters loaded by a CPL displaying a normal operation with tight voltage regulation and accurate power sharing, while maintaining an upper voltage bound at all times, even during transients.

References

[1] S. Parhizi, H. Lotfi, A. Khodaei, and S. Bahramirad, "State of the art in research on microgrids: A review," *IEEE Access*, vol. 3, pp. 890–925, 2015.

[2] H. Lotfi and A. Khodaei, "AC versus DC microgrid planning," *IEEE Transactions on Smart Grid*, vol. 8, no. 1, pp. 296–304, Jan 2017.

[3] S. E. Mhankale and A. R. Thorat, "Droop control strategies of DC microgrid: A review," in *2018 International Conference on Current Trends towards Converging Technologies (ICCTCT)*, March 2018, pp. 372–376.

[4] J. M. Guerrero, J. Matas, L. G. de Vicuna, N. Berbel, and J. Sosa, "Wireless-control strategy for parallel operation of distributed generation inverters," in *Proceedings of the IEEE International Symposium on Industrial Electronics, 2005. ISIE 2005.*, vol. 2, June 2005, pp. 845–850 vol. 2.

[5] J. M. Guerrero, L. Hang, and J. Uceda, "Control of distributed uninterruptible power supply systems," *IEEE Transactions on Industrial Electronics*, vol. 55, no. 8, pp. 2845–2859, Aug 2008.

[6] Y. A. I. Mohamed and E. F. El-Saadany, "Adaptive decentralized droop controller to preserve power sharing stability of paralleled inverters in distributed generation microgrids," *IEEE Transactions on Power Electronics*, vol. 23, no. 6, pp. 2806–2816, Nov 2008.

[7] A. Emadi, A. Khaligh, C. H. Rivetta, and G. A. Williamson, "Constant power loads and negative impedance instability in automotive systems: definition, modeling, stability, and control of power electronic converters and motor drives," *IEEE Transactions on Vehicular Technology*, vol. 55, no. 4, pp. 1112–1125, July 2006.

[8] D. Marx, P. Magne, B. Nahid-Mobarakeh, S. Pierfederici, and B. Davat, "Large signal stability analysis tools in DC power systems with constant power loads and variable power loads—a review," *IEEE Transactions on Power Electronics*, vol. 27, no. 4, pp. 1773–1787, April 2012.

[9] M. Cespedes, L. Xing, and J. Sun, "Constant-power load system stabilization by passive damping," *IEEE Transactions on Power Electronics*, vol. 26, no. 7, pp. 1832–1836, July 2011.

[10] A. Kwasinski and C. N. Onwuchekwa, "Dynamic behavior and stabilization of DC microgrids with instantaneous constant-power loads," *IEEE Transactions on Power Electronics*, vol. 26, no. 3, pp. 822–834, March 2011.

[11] W. Lee and S. Sul, "DC-link voltage stabilization for reduced dc-link capacitor inverter," *IEEE Transactions on Industry Applications*, vol. 50, no. 1, pp. 404–414, Jan 2014.

[12] P. Magne, B. Nahid-Mobarakeh, and S. Pierfederici, "DC-link voltage large signal stabilization and transient control using a virtual capacitor," in *2010 IEEE Industry Applications Society Annual Meeting*, Oct 2010, pp. 1–8.

[13] E. Coyne, D. Clarke, S. Heffernan, and B. Moane, "Designing ESD protection devices for ultrafast overvoltage events," *IEEE Transactions on Electron Devices*, vol. 66, no. 11, pp. 4850–4857, Nov 2019.

[14] F. Zhang, X. Duan, M. Liao, J. Zou, and Z. Liu, "Statistical analysis of switching overvoltages in UHV transmission lines with a controlled switching," *IET Generation, Transmission Distribution*, vol. 13, no. 21, pp. 4998–5004, 2019.

[15] P. D. F. Ferreira, P. M. S. Carvalho, L. A. F. M. Ferreira, and M. D. Ilic, "Distributed energy resources integration challenges in low-voltage networks: Voltage control limitations and risk of cascading," *IEEE Transactions on Sustainable Energy*, vol. 4, no. 1, pp. 82–88, Jan 2013.

[16] P. N. Vovos, A. E. Kiprakis, A. R. Wallace, and G. P. Harrison, "Centralized and distributed voltage control: Impact on distributed generation penetration," *IEEE Transactions on Power Systems*, vol. 22, no. 1, pp. 476–483, Feb 2007.

[17] Y. Ueda, K. Kurokawa, T. Tanabe, K. Kitamura, and H. Sugihara, "Analysis results of output power loss due to the grid voltage rise in grid-connected photovoltaic power generation systems," *IEEE Transactions on Industrial Electronics*, vol. 55, no. 7, pp. 2744–2751, July 2008.

[18] R. Tonkoski, L. A. C. Lopes, and T. H. M. El-Fouly, "Coordinated active power curtailment of grid connected PV inverters for overvoltage prevention," *IEEE Transactions on Sustainable Energy*, vol. 2, no. 2, pp. 139–147, April 2011.

[19] H. Chen, P. D. S. Assala, Y. Cai, and P. Yang, "Intelligent transient overvoltages location in distribution systems using wavelet packet decomposition and general regression neural networks," *IEEE Transactions on Industrial Informatics*, vol. 12, no. 5, pp. 1726–1735, Oct 2016.

[20] A. C. Braitor, G. C. Konstantopoulos, and V. Kadirkamanathan, "Current-limiting droop control design and stability analysis for paralleled boost converters in DC microgrids," *IEEE Transactions on Control Systems Technology*, pp. 1–10, 2020.

[21] G. C. Konstantopoulos and P. R. Baldivieso-Monasterios, "State-limiting PID controller for a class of nonlinear systems with constant uncertainties," *International Journal of Robust and Nonlinear Control*, vol. n/a, no. n/a, 2019. [Online]. Available: https://onlinelibrary.wiley.com/doi/abs/10.1002/rnc.4853

[22] C. D. Meyer, *Matrix Analysis and Applied Linear Algebra*. Philadelphia: Society for Industrial and Applied Mathematics, 2000.